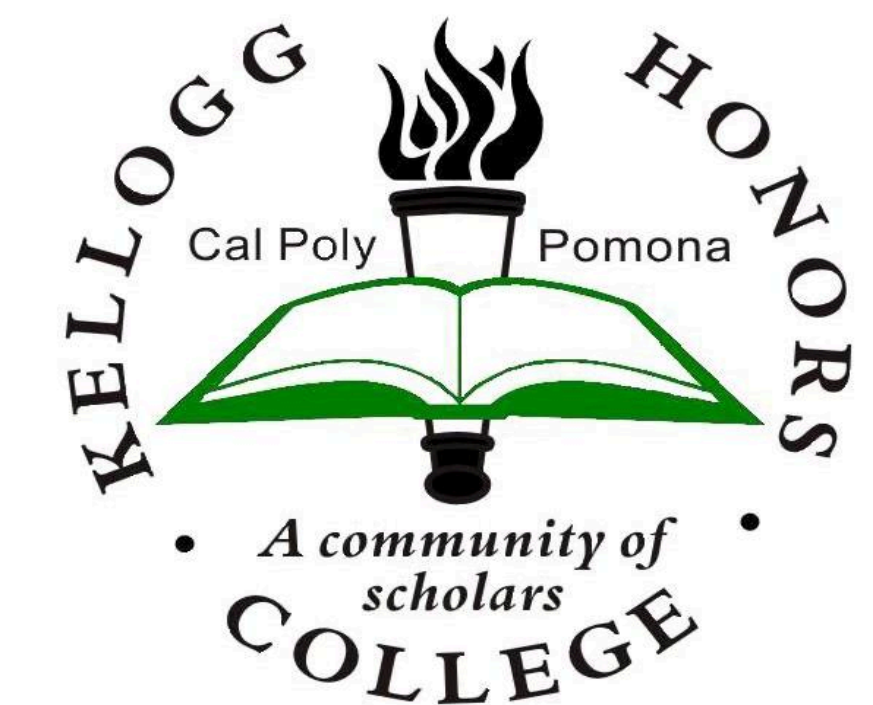


System Identification and Controller Optimization of Coaxial Quadrotor UAV in Hover



Sung Hyeok Cho
Aerospace Engineering
Mentor: Dr. Subodh Bhandari
Kellogg Honors College Capstone Project



Abstract

With relatively little study done on the stability and control of coaxial multirotor UAV configurations, more data is required to accurately assess the benefits of the coaxial configuration compared to traditional multirotor configurations. To identify the effect of the coaxial configuration on a multirotor's hover/low speed dynamics, system identification of the 3DR X8+ aircraft, a coaxial quadrotor, via frequency domain system identification techniques were performed. The obtained dynamics were then used to design and optimize an Attitude Command/Attitude Hold control law utilizing the Explicit Model Following architecture.

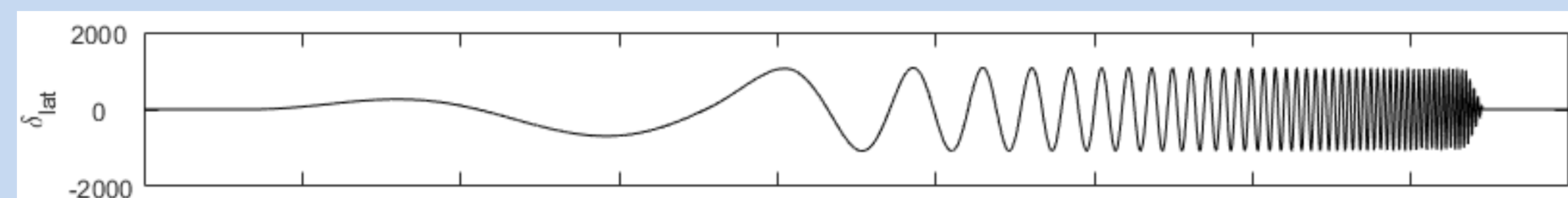
Flight Vehicle

The aircraft tested was the 3DR X8+, a coaxial quadrotor. The vehicle was modified in order to facilitate data collection and flight testing. It is equipped with a PixHawk 2.1 flight controller, operating a modified ArduCopter firmware. The system logs angular rates, velocity estimations, attitudes, pilot input, and mixer input at 100 Hz. In addition, the system allows for injection of custom pilot inputs as well as mixer inputs, which is used for both system identification and turbulence rejection data collection.



Flight Testing

The flight tests were conducted with the ArduCopter's stock "Stabilize" mode control system, with frequency sweep and doublet maneuvers injected into the pilot input. The aircraft was swept from 0.5 rad/s to 60 rad/s over 60 seconds while in hover in each axis. Each flight data log included 5 seconds of trim condition before and after the maneuver to allow for removal of sensor bias. The resulting flight data was then processed via a MATLAB script which performed unit conversion, data truncation, and processed the data to be compatible with the CIFER® software package.

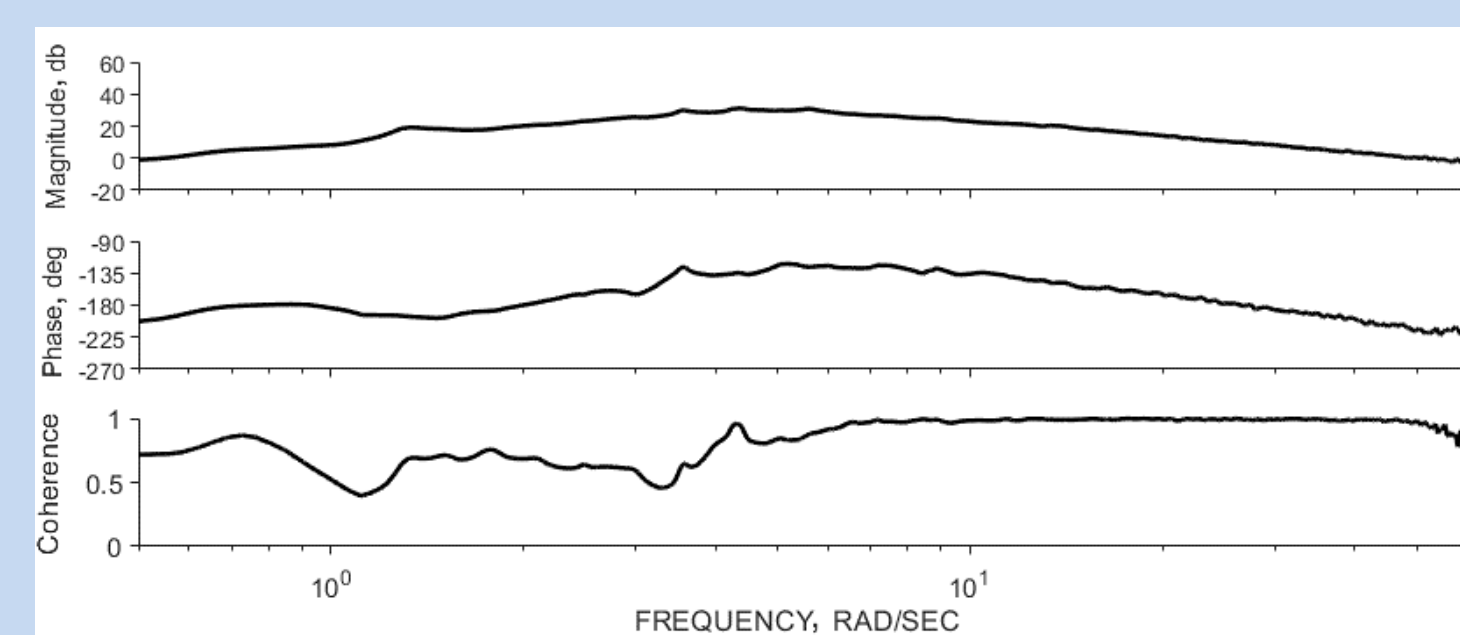


Frequency Response

The frequency responses of each axis were obtained from the frequency sweeps using CIFER®'s FRESPID module. Body translational accelerations were reconstructed via the following equations:

$$\begin{aligned} \dot{u} &= a_{x_{cg}} - W_0 q + V_0 r - (g \cos \theta_0) \theta \\ \dot{v} &= a_{y_{cg}} - U_0 q + W_0 p + (g \cos \theta_0) \phi \\ \dot{w} &= a_{z_{cg}} - V_0 p + U_0 q - (g \sin \theta_0) \theta \end{aligned}$$

Through MISOSA and COMPOSITE modules of CIFER®, effects of cross-correlated inputs were removed, and composite windowing was performed to gain more accurate frequency responses across a wider frequency range. Coherence is high across most of the frequency range of interest, showing excellent linearity and high signal to noise ratio in the data.



System Identification

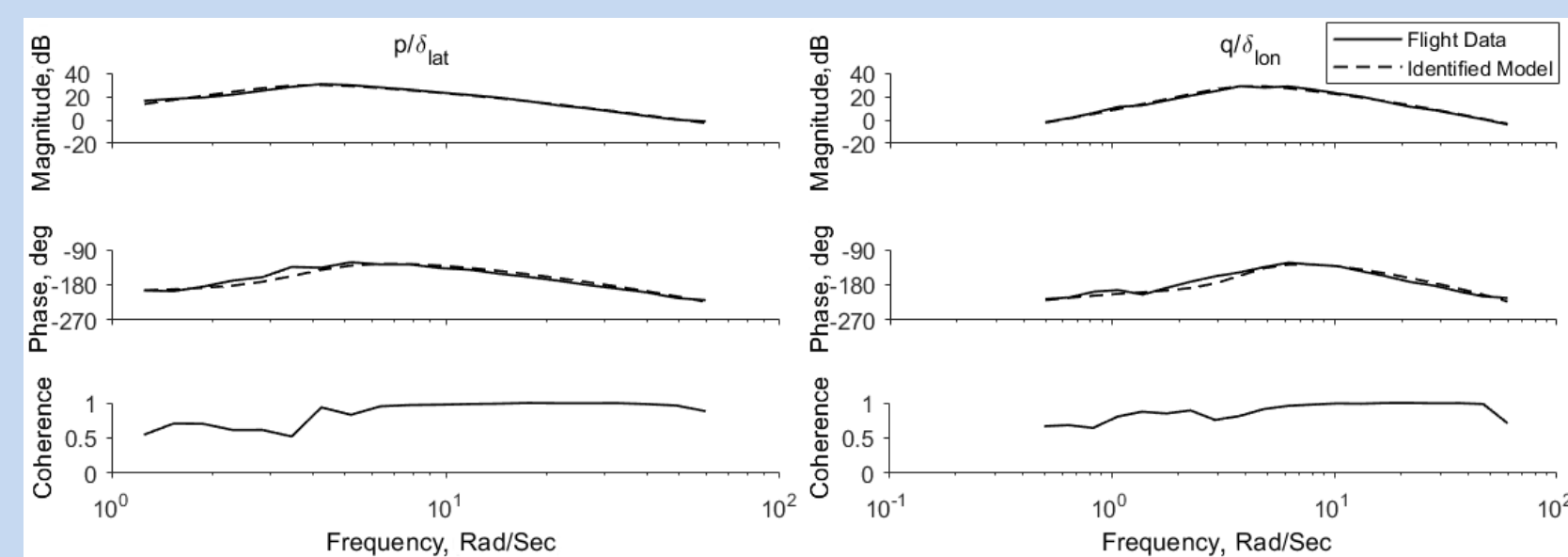
In order to obtain initial estimates of parameters for state-space model identification, lower-order transfer function models of vehicle dynamics were identified from the dominant on-axis frequency responses. This was accomplished using the NAVFIT module of CIFER®.

$$\begin{aligned} \frac{p}{\delta_{lat}} &= \frac{L_{lat} s (s - Y_v) e^{-\tau_{lat} s}}{s^3 - Y_v s^2 - L_v g}, & \frac{q}{\delta_{lon}} &= \frac{M_{lon} s (s - X_u) e^{-\tau_{lon} s}}{s^3 - X_u s^2 + M_u g} \\ \frac{a_z}{\delta_{col}} &= Z_{col} e^{-\tau_{col} s}, & \frac{r}{\delta_{ped}} &= \frac{N_{ped} e^{-\tau_{ped} s}}{s - N_r} \end{aligned}$$

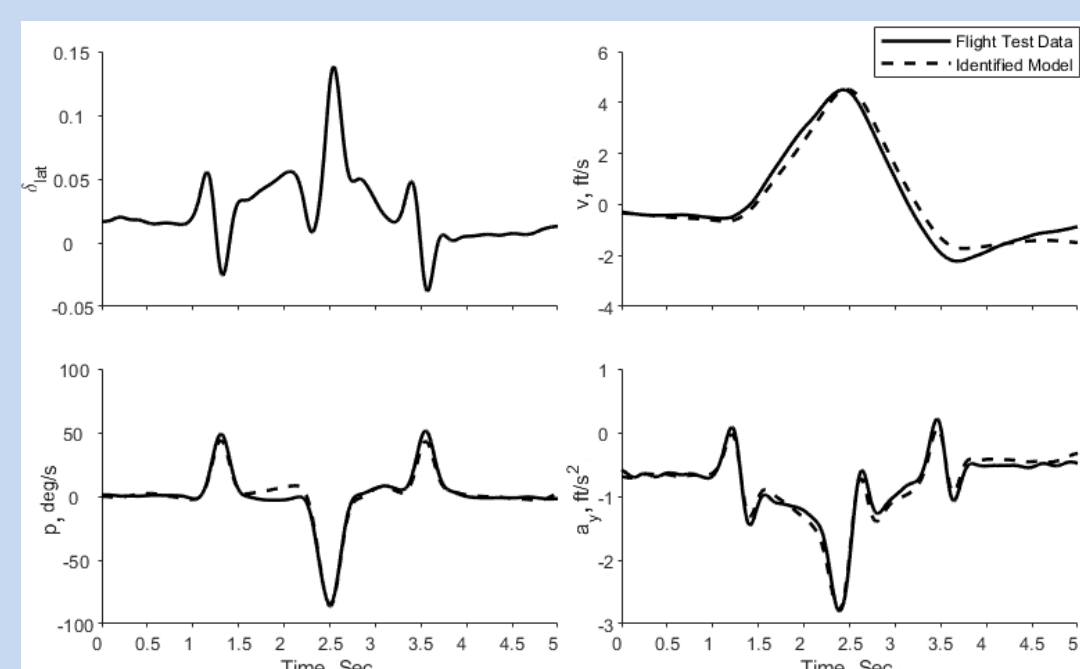
The identification was performed in the frequency range of 0.5 – 15 rad/s. The cost function (J) of each individual model were all below 40 with exception of yaw axis, which had a cost function of 77.8. The state-space identification was accomplished using the DERIVID module of CIFER®. With the initial values of parameters identified via NAVFIT, a state-space model was identified from the frequency responses obtained above. Through elimination of parameters with high insensitivity or high uncertainty bounds, the model was reduced until no extraneous parameters were left.

$$\begin{bmatrix} \dot{u} \\ \dot{v} \\ \dot{w} \\ \dot{p} \\ \dot{q} \\ \dot{r} \\ \dot{\theta} \\ \dot{\phi} \\ \dot{\psi} \\ \delta_{lat} \\ \delta_{lon} \\ \delta_{col} \\ \delta_{ped} \end{bmatrix} = \begin{bmatrix} X_u & 0 & 0 & 0 & 0 & 0 & 0 & 0 & 0 & 0 & 0 & 0 & 0 \\ 0 & Y_v & 0 & 0 & 0 & 0 & 0 & 0 & 0 & 0 & 0 & 0 & 0 \\ 0 & 0 & Z_w & 0 & 0 & 0 & 0 & 0 & 0 & 0 & 0 & 0 & 0 \\ 0 & 0 & 0 & L_v & 0 & 0 & 0 & 0 & 0 & L_{lat} & 0 & 0 & 0 \\ 0 & 0 & 0 & 0 & 0 & 0 & 0 & 0 & 0 & 0 & M_{lon} & 0 & 0 \\ 0 & 0 & 0 & 0 & 0 & 0 & N_r & 0 & 0 & 0 & 0 & N_{ped} & -lag + lead \\ 0 & 0 & 0 & 0 & 0 & 0 & 0 & 0 & 0 & 0 & 0 & 0 & 0 \\ 0 & 0 & 0 & 0 & 0 & 0 & 0 & 0 & 0 & 0 & 0 & 0 & 0 \\ 0 & 0 & 0 & 0 & 0 & 0 & 0 & 0 & 0 & 0 & 0 & 0 & 0 \\ 0 & 0 & 0 & 0 & 0 & 0 & 0 & 0 & 0 & 0 & 0 & 0 & 0 \\ 0 & 0 & 0 & 0 & 0 & 0 & 0 & 0 & 0 & 0 & 0 & 0 & 0 \\ 0 & 0 & 0 & 0 & 0 & 0 & 0 & 0 & 0 & 0 & 0 & 0 & 0 \\ 0 & 0 & 0 & 0 & 0 & 0 & 0 & 0 & 0 & 0 & 0 & 0 & 0 \end{bmatrix} \begin{bmatrix} u \\ v \\ w \\ p \\ q \\ r \\ \theta \\ \phi \\ \psi \\ \delta_{lat} \\ \delta_{lon} \\ \delta_{col} \\ \delta_{ped} \end{bmatrix} + \begin{bmatrix} 0 & 0 & 0 & 0 & 0 & 0 & 0 & 0 & 0 & 0 & 0 & 0 & 0 \\ 0 & 0 & 0 & 0 & 0 & 0 & 0 & 0 & 0 & 0 & 0 & 0 & 0 \\ 0 & 0 & 0 & 0 & 0 & 0 & 0 & 0 & 0 & 0 & 0 & 0 & 0 \\ 0 & 0 & 0 & 0 & 0 & 0 & 0 & 0 & 0 & 0 & 0 & 0 & 0 \\ 0 & 0 & 0 & 0 & 0 & 0 & 0 & 0 & 0 & 0 & 0 & 0 & 0 \\ 0 & 0 & 0 & 0 & 0 & 0 & 0 & 0 & 0 & 0 & 0 & 0 & 0 \\ 0 & 0 & 0 & 0 & 0 & 0 & 0 & 0 & 0 & 0 & 0 & 0 & 0 \\ 0 & 0 & 0 & 0 & 0 & 0 & 0 & 0 & 0 & 0 & 0 & 0 & 0 \\ 0 & 0 & 0 & 0 & 0 & 0 & 0 & 0 & 0 & 0 & 0 & 0 & 0 \\ 0 & 0 & 0 & 0 & 0 & 0 & 0 & 0 & 0 & 0 & 0 & 0 & 0 \\ 0 & 0 & 0 & 0 & 0 & 0 & 0 & 0 & 0 & 0 & 0 & 0 & 0 \\ 0 & 0 & 0 & 0 & 0 & 0 & 0 & 0 & 0 & 0 & 0 & 0 & 0 \\ 0 & 0 & 0 & 0 & 0 & 0 & 0 & 0 & 0 & 0 & 0 & 0 & 0 \end{bmatrix} \begin{bmatrix} \delta_{lat}(t - \tau_{lat}) \\ \delta_{lon}(t - \tau_{lon}) \\ \delta_{col}(t - \tau_{col}) \\ \delta_{ped}(t - \tau_{ped}) \end{bmatrix}$$

The final cost function was $J_{avg} \approx 44$. The low cost function and Cramer-Rao bounds indicate that the model is highly accurate and that the identified parameters are reliable. As shown by the model's frequency response on the right, the model response very closely follows the flight data.



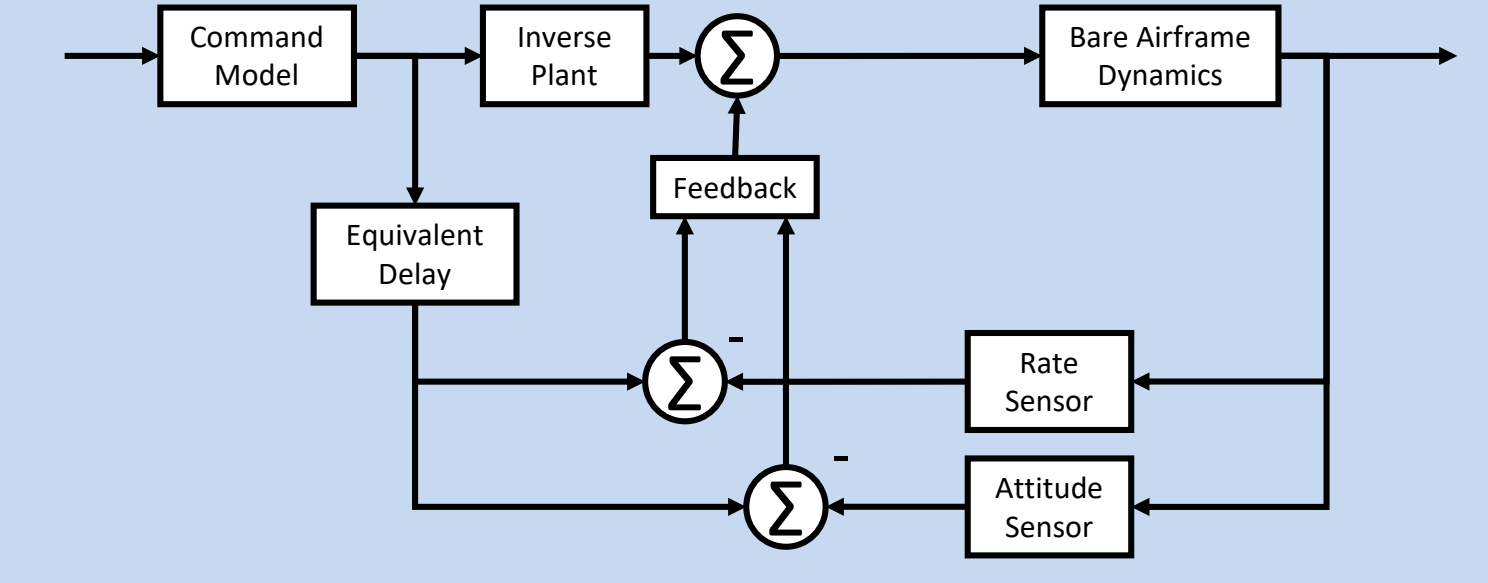
As the model was identified entirely in the frequency domain, time domain verification via a different maneuver is necessary to ensure good predictive accuracy in the time domain. The time domain identification was accomplished via the VERIFY module of CIFER®, in which a flight test data of a doublet maneuver in each axis was used to verify the model. The verification shows that the identified model is capable of tracking the flight test data closely, even in maneuvers where attitude reaches nonlinear ranges.



Control System Design

The control law architecture chosen to design the optimized control system was Explicit Model Following (EMF) architecture. EMF is considered a "two degree of freedom" feedback system, where pilot command response characteristics can be designed separately from feedback response. The EMF architecture was chosen as it is widely used in many full-scale aircraft control systems.

In an EMF architecture, command model outputs a desired aircraft response from pilot input, and the inverse plant uses a lower order model of the bare airframe dynamics to generate a feed-forward control signal. Equivalent delay is used to synchronize the command model output with the feedback signal from the higher-order dynamics. The feedback loop is used for gust rejection, correction of any inverse plant errors, and ensure robustness.



Inverse plants were obtained by rearranging the low order transfer function models to produce actuator signal as a function of aircraft attitude. The inverse plant for each axis is as follows, with parameters taken directly from the identified model.

$$\begin{aligned} \delta_{lat_{ff}} &= (\dot{p}_{cm} - \frac{L_{v0}}{s - Y_v} \Phi_{cm}) / L_{lat}, & \delta_{lon_{ff}} &= (\dot{q}_{cm} + \frac{M_{u0}}{s - X_u} \theta_{cm}) / M_{lon} \\ \delta_{col_{ff}} &= a_{z_{cm}} / Z_{col}, & \delta_{ped_{ff}} &= \frac{\dot{r}_{cm} - N_r r_{cm}}{N_{ped}} * \frac{N_{ped}}{lead + s + 1} \end{aligned}$$

Control Optimization

Optimization of the control law was accomplished using the CONDUIT® software package. CONDUIT® optimizes a given set of design parameters against a set of handling quality "specs," or specifications plots derived from various requirements such as ADS-33. Handling quality specs provided by the built in libraries were utilized, with modified crossover frequency specs and disturbance rejection specs. Each spec was then assigned a constraint type, which indicated the priority of meeting Level 1 handling quality requirements: hard, soft, and objective. Objective specs are optimized last to achieve all of the specs with minimum overdesign, reaching the Pareto optimum.

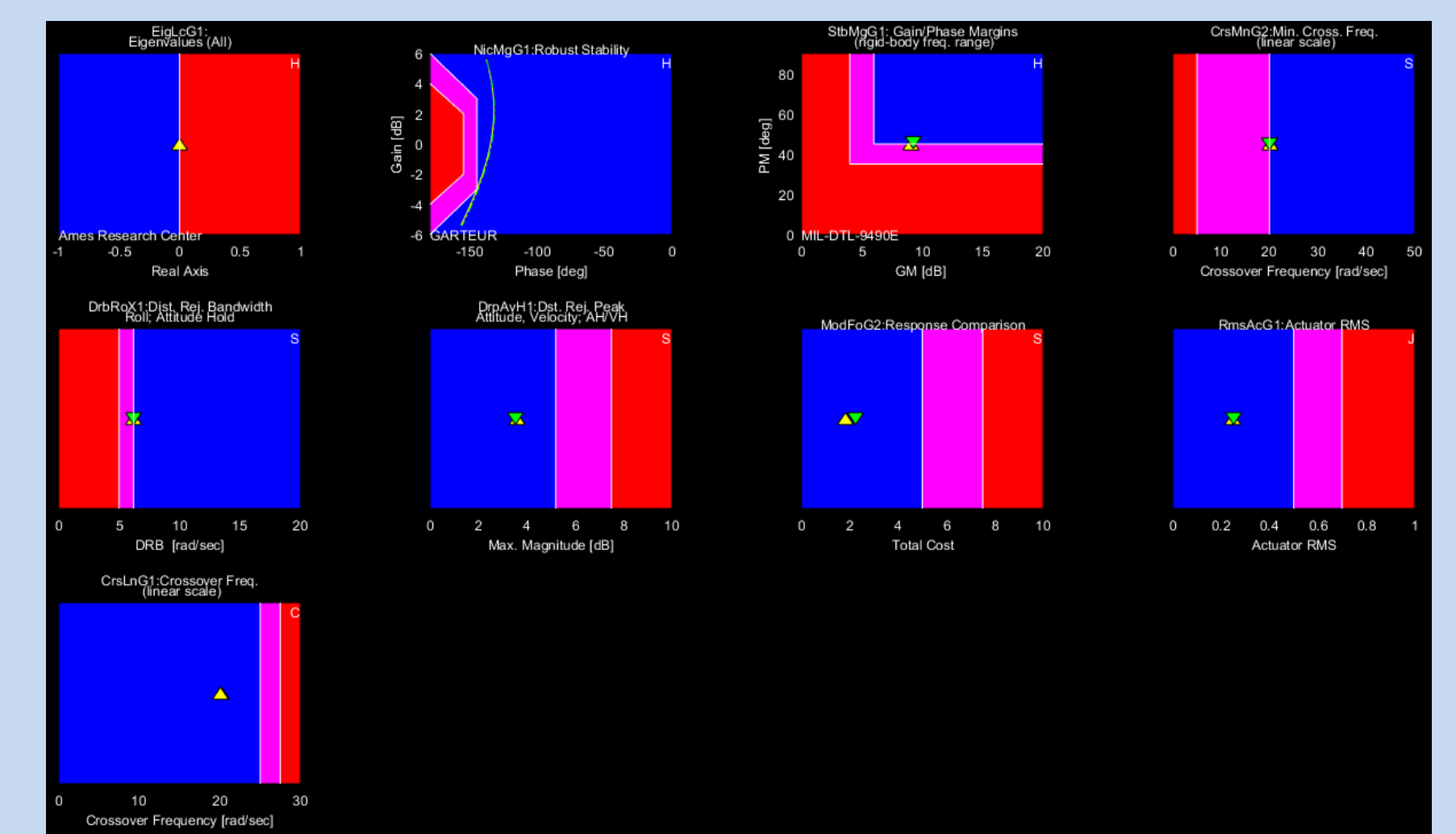
The primary objective of optimization was increase in disturbance rejection bandwidth and reduction in actuator usage. In addition, the integrator gains were fixed to be 2/5th of the proportional gain, as the optimization process can deem the integrator gains to be insensitive and drive them to undesirable values. For this optimization, minimum crossover frequency of 20 rad/s was chosen.

During optimization, it was discovered that lead and lag compensators were required to reach desired performance. The lead lag compensators are shown.

$$\text{Longitudinal, Lateral Axis: } \frac{(s+3)(s+4)}{(s+72)(s+0.1)}$$

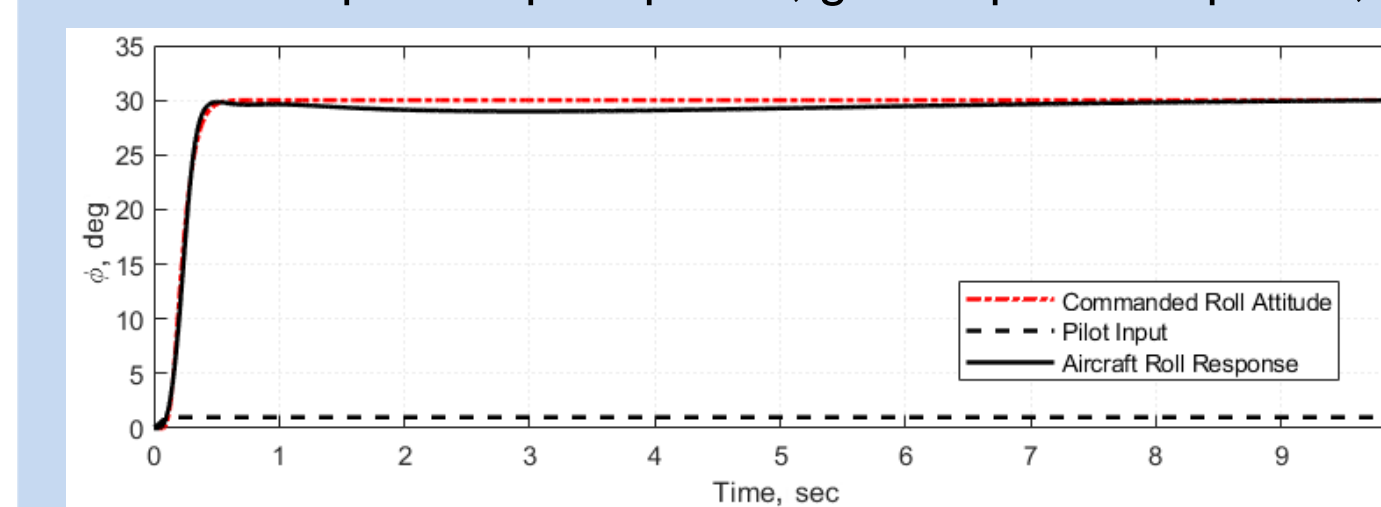
$$\text{Collective Axis: } \frac{s+3}{s+48}$$

$$\text{Directional Axis: } \frac{s+10}{s+24}$$

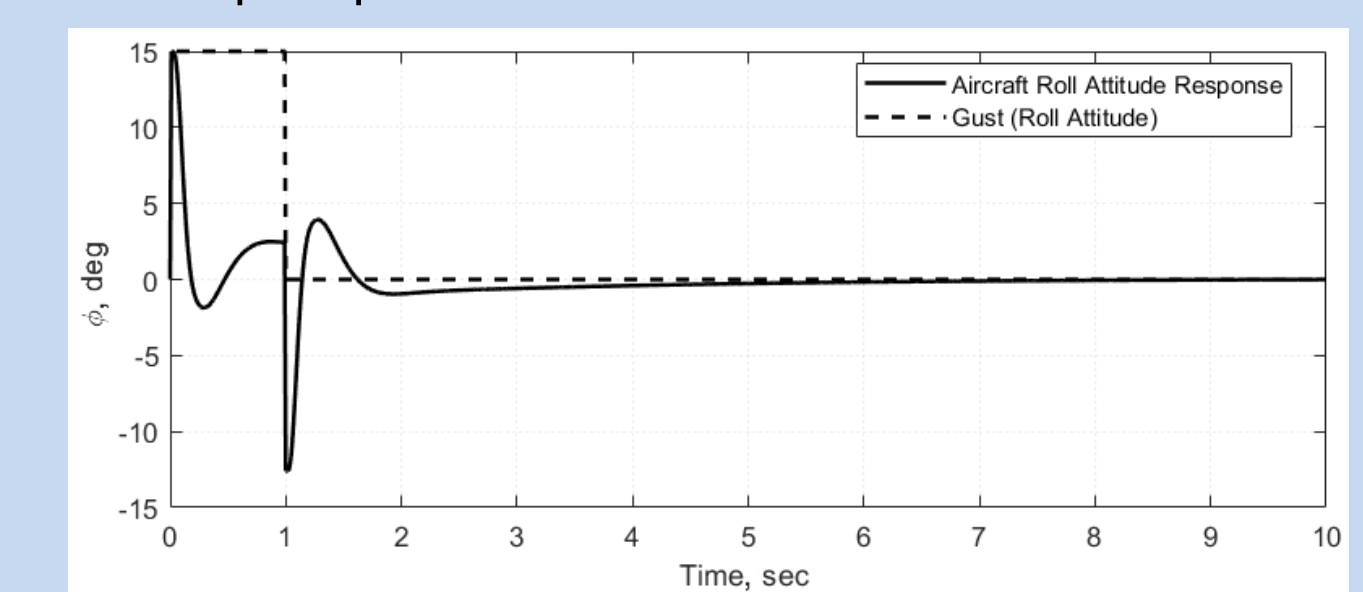


A sample optimization result for lateral and longitudinal axis is shown on the right. The blue indicates level 1 handling quality, pink level 2, and red level 3. The optimized system lies on the border between level 1 and 2, indicating that it has reached the Pareto optimum.

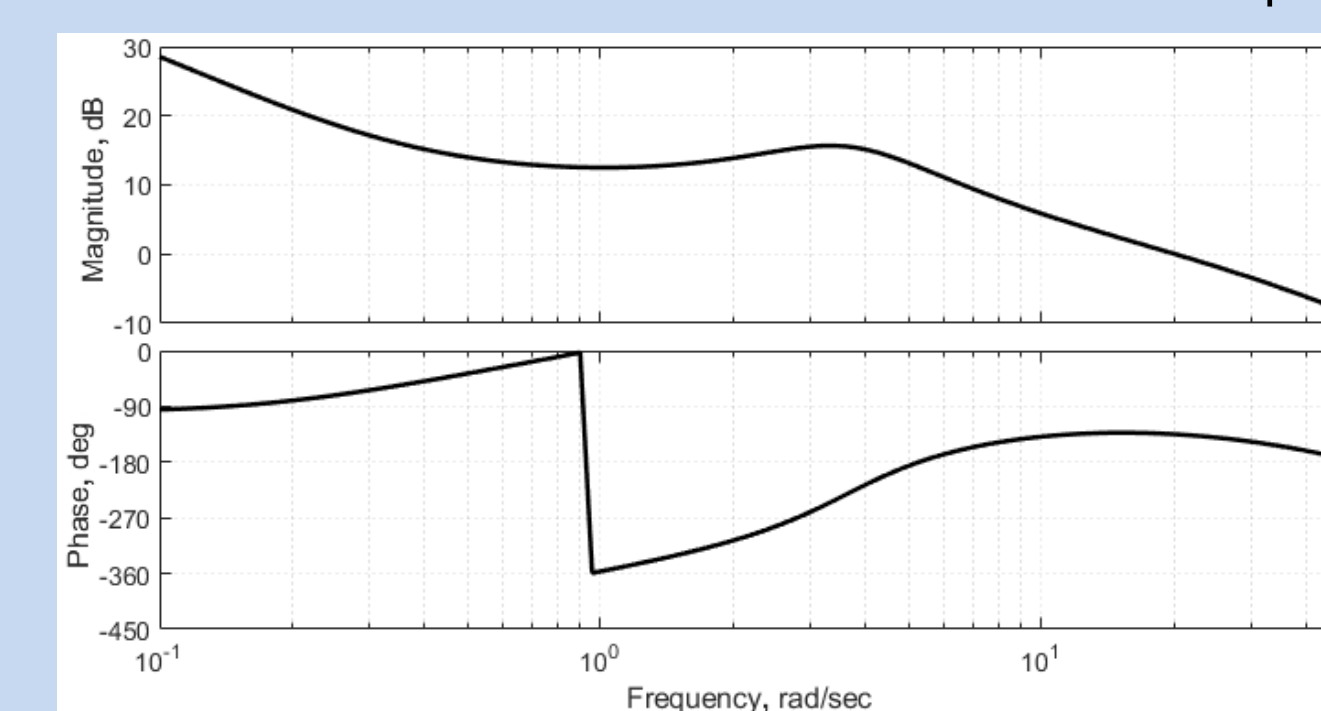
Lateral axis pilot step response, gust impulse response, and broken loop response is shown below.



Pilot Step Response



Gust Impulse Response



Broken Loop Response

Conclusions

The 3DR X8+'s hover/low-speed bare airframe dynamics was identified using the CIFER® software package. The identified model was shown to be accurate to the frequency range of 0.5 – 60 rad/s, and the accuracy of the model was verified in the time domain using a doublet flight data. The identified model's angular response is dominated by L_v and M_u derivatives, with traditional angular damping derivatives having negligible contribution to the dynamics. The X8+'s bare airframe dynamics was then utilized to design and optimize an Attitude Command/Attitude Hold control system using the Explicit Model Following architecture. Optimization was conducted via the CONDUIT® software package, which optimized the control system to its Pareto optimum via reducing actuator usage while retaining Level 1 handling qualities defined by the handling quality specs.

Special thanks to Army Aviation Development Directorate, Frank C. Sanders, Mark B. Tischler, and Kenny K. Cheung, and Universities Space Research Association for assisting with this research. This poster was adapted from research presented at SciTech Forum 2019 under "System Identification and Controller Optimization of Coaxial Quadrotor UAV in Hover."